American Journal of Energy Research, 2025, Vol. 13, No. 1, 19-25
Available online at http://pubs.sciepub.com/ajer/13/1/3
Published by Science and Education Publishing
DOI:10.12691/ajer-13-1-3

Modeling and Simulation of A Hydraulic Storage System Powered By A Photovoltaic Generator

Haïdara Savadogo[1,*], Eric Korsaga[1], Toussaint Tilado Guingane[1,2], Dominique Bonkoungou[1,2], Zacharie Koalaga[1]

[1]Laboratoire de Matériaux et Environnement (LAME), Université Joseph KI-ZERBO, 03 BP 7021 Ouagadougou, Burkina Faso
[2]Laboratoire de Sciences et Technologies (LaST), Université Thomas SANKARA, 12 BP 417 Saaba, Burkina Faso
*Corresponding author: sava86haidara@gmail.com

Received February 15, 2025; Revised March 16, 2025; Accepted March 23, 2025

Abstract Due to its arid nature and the availability of a large amount of sunlight in the Sahel, water pumping via solar photovoltaic systems can play a very important role in the agricultural and industrial sectors for rural communities in developing countries. However, this type of system could be directly influenced by the variability of sunshine, which fluctuates from day to day and from season to season. To better understand these difficulties, we propose to carry out a theoretical study to improve the performances of a water pumping system comprising a photovoltaic field, an asynchronous motor connected to a surface centrifugal pump and a water reservoir. The aim is to model and simulate the system using Matlab/Simulink software using a dynamic method. This work highlights the evolution of motor pump performance over time, in relation to the intensity of solar lighting. This dynamic method provides a better understanding of immediate changes in performance. The success of this modeling opens the way to practical applications, particularly in remote regions and rural areas where access to water and the electricity grid is limited, environmentally-friendly energy economy.

Keywords: *Photovoltaic generator, Asynchronous motor, hydraulic storage, Modeling, Simulation*

Cite This Article: Haïdara Savadogo, Eric Korsaga, Toussaint Tilado Guingane, Dominique Bonkoungou, and Zacharie Koalaga, "Modeling and Simulation of A Hydraulic Storage System Powered By A Photovoltaic Generator." *American Journal of Energy Research*, vol. 13, no. 1 (2025): 19-25. doi: 10.12691/ajer-13-1-3.

1. Introduction

In many rural areas of the world, access to a reliable source of water remains a major challenge, holding back economic and social development [1]. So, in remote rural areas of Africa, water collection is still largely carried out manually, a task that requires a great deal of time and effort [2]. The motorization of pumps represents a significant advance, reducing drudgery and freeing up time for other essential activities [3]. Among the various alternatives, photovoltaic solar pumping is economically competitive and a promising solution [4]. The most widely used solar pumping system is the so-called "run-of-solar" system, as it enables photovoltaic energy to be used directly from solar photovoltaic modules, without the need for conversion or storage devices. Several models focusing on sizing and modeling the operation of each component of the photovoltaic pumping system have been created and experimentally tested to evaluate the performance of photovoltaic pumping systems [5-12]. S. Meunier [5] presents a study on the design, modeling and experimental validation of a photovoltaic pumping system, intended to supply water to an isolated rural community to meet drinking water needs while harnessing a renewable energy source adapted to the local context. A. I. Imadan [6] and D. Abbes [7] discuss the sizing and design of a solar photovoltaic pumping system and propose a sustainable and economical solution to meet farmers' water needs, taking advantage of the abundance of solar energy in the region. R. Nisha [8] offers a review of photovoltaic-powered water pumping systems using brushless DC motors and examines the advances, technologies and challenges associated with these systems in various application contexts. T. T. Assefa T. F. Adametie [9] evaluates the effectiveness and impact of using the Solar MajiPump, a solar-powered pump, in irrigation and agricultural systems in Ethiopia to promote sustainable agriculture and solve the problems associated with limited access to water for farmers in rural areas. R. B. Silva [12] analyzes the water balance and technical-financial performance of irrigation systems in cassava cultivation to understand how optimized water management can improve yields and profitability of this crop, while preserving water resources.

However, these studies approach a method of examination or problem-solving that focuses on a specific state, without considering progress or changes over time. This static study, while providing some elements, remains insufficient, limiting overall understanding of dynamic functioning and adaptation to variations in climatic and water conditions.

Our research is distinguished by the development of a model that simulates the whole system, the impact of fluctuations in solar radiation on the performance of

photovoltaic solar pumping systems in real environments characterized by dynamic variations.

With this in mind, this article studies the integration of a hydraulic storage system connected to a photovoltaic generator. Following the introduction, we present the system modeling in section 2. Section 3 presents and discusses the results obtained. The final section concludes this work.

2. System Modeling

The water pumping system studied consists of a photovoltaic array made up of 35 strings of 8 modules with 215 Wp power in series, a boost converter, a three-phase inverter, a motor pump and a water storage tank. The corresponding block diagram is shown in Figure 1.

2.1. Photovoltaic Array Model

The photovoltaic field can be modeled by the equation (1) [13].

$$P_{Max} = \eta_{PV}.A_{PV}.G \quad (1)$$

where η_{pv} is the module efficiency, A_{PV} the module area (m²) and G the illuminance incident on the module plane (W/m²). In relation (1), η_{pv} is the overall module efficiency, given by equation (2) [13]:

$$\eta_{PV} = \eta_r.\eta_{PC}.\left[1-\beta_t(T_{Cell}-T_{cel\_r}\right] \quad (2)$$

where η_r is the module efficiency under standard conditions, ηpc is the degradation factor and in this study it will be equal to 0.9.

T_{cel_r} is the cell temperature (Standard conditions) equal to 25° C. T_{cell} is the cell temperature, which varies as a function of illuminance and ambient temperature, according to the following linear relationship (3) [13,14,15]. It is given by the relation (3):

$$T_{cell} = T_a + (NOCT - 20°C).\left(\frac{G_\beta}{800}\right) \quad (3)$$

where NOCT is the cell's operating temperature. It is defined as the temperature the cell reaches in its open-circuit module, under sunlight at G_β = 800 W/m², with an ambient temperature of 20°C and a wind speed of 1 m/s. Various NOCT values are used in the literature. In this article, we consider the typical NOCT value to be 45°C.

β_t in the relation (2) is the coefficient of influence of photovoltaic cell temperature on module efficiency. Its value ranges from 0.004/ºC to 0.006/ºC [16]. The parameters for standard conditions ($Tcel\_r$ and η_r) and the coefficient β_t are provided by PV module manufacturers. In this work, we chose monocrystalline silicon modules with η_r efficiencies varying between 10 and 14% [17]. Here η_r will be set to 14% and the coefficient β_t will be taken equal to 0.0048/ºC. The Matlab/Simulink environment will be used to represent the photovoltaic field model defined using relationship (1).

2.2. Converter Models

Converters have been studied and several models have been developed by different authors [17,18,19]. Many experts believe that their performance remains the same in general [16,19]. As a result, the boost chopper and inverter are considered to be complex pieces of equipment whose function affects power. In simple terms, it's a question of measuring the efficiency of the transformation carried out from the outset. In our work, they are all represented by their identical ηboost and ηond efficiencies, taken to be egal to 0.90 each.

2.3. Motor Pump Model

The motor-driven pump consists of a three-phase motor driving a centrifugal pump.

2.3.1. Asynchronous Motor Model

The asynchronous motor is represented using the conventional equivalent circuit shown in Figure 2 [20].

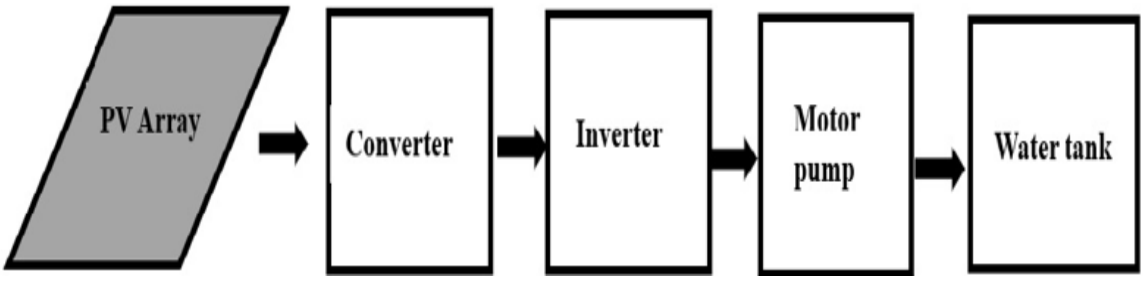

Figure 1. Pumping system block diagram

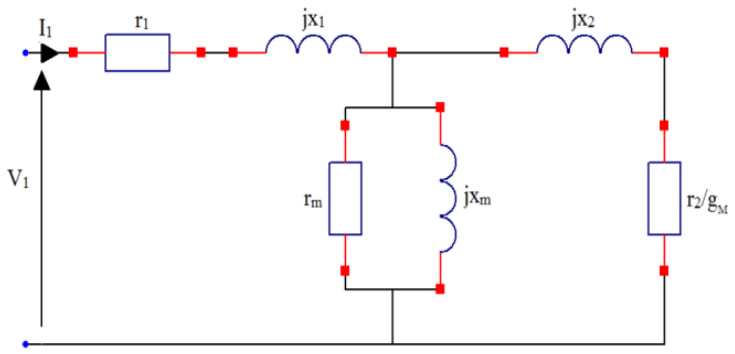

Figure 2. Asynchronous motor equivalent diagram

The input electrical power is then given by the following equation (4):

$$P_a = 3.V_1.I_1.\cos\varphi \tag{4}$$

By replacing I_1 in equation (4), the input electrical power is expressed by the relation (5):

$$P_a = 3.\frac{V_1^2}{Z_{eq}}.\cos\varphi \tag{5}$$

where Z_{eq} is the equivalent complex impedance of the equivalent circuit given by the relation (6):

$$\overline{Z_{eq}} = r_1 + jX_1 + \frac{r_m.x_m.\left(-x_2 + \frac{j.r_2}{g_M}\right)}{\left(\frac{r_m.r_2}{g_M} - x_m.x_2\right) + j\left(\frac{x_m.r_2}{g_M} + r_m.x_2 + x_m.r_m\right)} \tag{6}$$

However, the electromagnetic torque can be calculated using the following expression (7) [21,22]:

$$C_{em} = 3.p.\left(\frac{V_1}{\omega_s}\right)^2.\frac{\omega_{sl}.\frac{x_m^2}{r_2}}{\left[r_1 - \frac{\omega_{sl}}{\omega_s.r_2}\left(x_{11}.x_{22} - x_m^2\right)\right]^2 + \left[x_{11} + \frac{\omega_{sl}.r_1.x_{22}}{\omega_s.r_2}\right]^2} \tag{7}$$

It's an expression that involves relationships between the system's voltage, frequency, reactances, and impedance elements.

The mechanical equilibrium between the motor and pump is given by the following mechanical equation (8) [21]:

$$C_{em} = C_r + C_o\omega \tag{8}$$

where C_{em} is the electromagnetic torque, C_r the pump resistive torque, C_o is the motor viscous friction coefficient, and ω the rotational speed.

On the other hand, the resistive torque is given by the equation (9) [22]:

$$C_r = k\omega^2 + C_{rs} \tag{9}$$

where Crs is the static resistive torque (very low) and k a characteristic coefficient of the pump and ω speed of rotation of the asynchronous motor. Replacing equation (9) in (8) and equating it with equation (7) assuming negligible static resistive torque (Crs = 0), we obtain the following relationship (10):

$$k\omega^2 + C_o\omega = 3.p.\left(\frac{V_1}{\omega_s}\right)^2.\frac{\omega_{sl}.\frac{x_m^2}{r_2}}{\left[r_1 - \frac{\omega_{sl}}{\omega_s.r_2}\left(x_{11}.x_{22} - x_m^2\right)\right]^2 + \left[x_{11} + \frac{\omega_{sl}.r_1.x_{22}}{\omega_s.r_2}\right]^2} \tag{10}$$

Solving this second-degree equation gives us the following positive solution (11):

$$\omega = \frac{-C_o + \sqrt{C_o^2 + 2{,}05.10^{-2}.k.P_a}}{2.k} \tag{11}$$

The Matlab/Simulink environment will be used to represent the asynchronous motor model defined using the following positive solution (11).

2.3.2. Pump Model

To model the pump, we'll use pump similarity laws [23-25]. The performance of a centrifugal pump (Q_N, H_N, and P_N) for a given rotational speed ω_N (rad/s) can be determined with the aid of similarity laws using the following equations (12) to (14):

$$Q = Q_N\left(\frac{\omega}{\omega_N}\right) \tag{12}$$

$$H = H_N\left(\frac{\omega}{\omega_N}\right)^2 \tag{13}$$

$$P = P_N\left(\frac{\omega}{\omega_N}\right)^3 \tag{14}$$

where water flow Q and Q_N correspond to velocity ω and velocity ω_N ; total head H and H_N correspond to velocity ω and velocity ω_N ; and mechanical power P and P_N correspond to velocity ω and velocity ω_N.

2.4. Water Reservoir Model

The reservoir model is used to calculate the potential energy of the water accumulated during the storage phase. The potential energy of the reservoir at altitude Z_1 is given by relationship (15):

$$E_P = MgZ_1 \quad (15)$$

where M is the mass of water stored in kg, g is the acceleration ((9.80 m)⁄s²) and Z_1 (m) is the altitude of the reservoir invert.

The evolution of water volume in the reservoir over time is described by relationship (16):

$$V_{O1} = \int_{t_0}^{t_1} Q(t).dt + V_0 \quad (16)$$

where Q is the pumping volume flow rate, t_o is the simulation start time (pump start), t_1 is the simulation end time (pump stop) and V_o is the volume of unusable water. Initially, the variation in the mass of water in the reservoir is obtained by multiplying expression (16) by ρ and obtaining relation (17):

$$M(t) = \rho(\int_{t_0}^{t_1} Q(t).dt + V_0) \quad (17)$$

In the second step, the variation of the potential energy in the reservoir is obtained by multiplying expression (17) by gZ_1 and obtaining relation (18):

$$E_P(t) = M(t)gZ_1 = gZ_1\rho(\int_{t_0}^{t_1} Q(t).dt + V_0) \quad (18)$$

The Matlab/Simulink environment will be used to represent the water volume and potential energy model defined using relations (16) and (18).

2.5. Modeling in Matlab/Simulink

Figure 3 illustrates four distinct blocks, taking solar irradiation and ambient temperature as inputs, and producing water volume and potential energy as outputs. It highlights the interconnection between these input variables and their transformation into outputs through the various calculation steps. The figure also shows the complete model of the proposed pumping system, implemented in Matlab/Simulink.

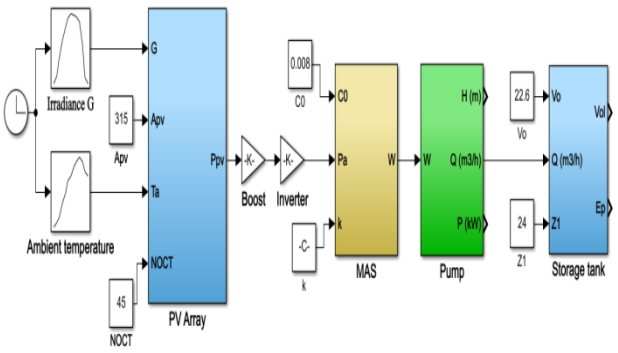

Figure 3. Matlab/Simulink model of the photovoltaic pumping

Figure 4 shows the photovoltaic field, with solar irradiance as input and PV field power as output.

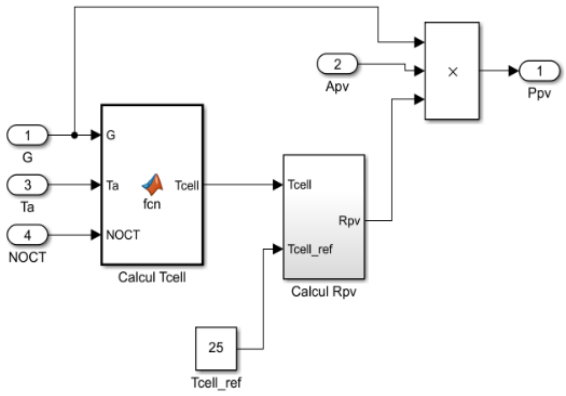

Figure 4. Photovoltaic field diagram

Figure 5 shows the calculation diagram for the asynchronous machine, where the input is the power input and the output is the motor shaft speed.

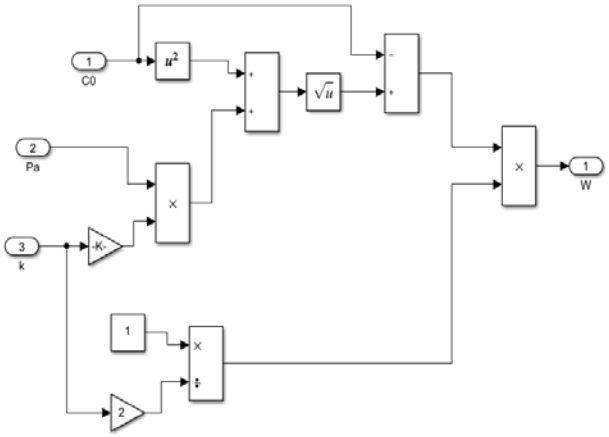

Figure 5. Asynchronous motor flow chart

Figure 6 shows the calculation diagram for the pump, where the input is the pump speed and the output is the water flow rate.

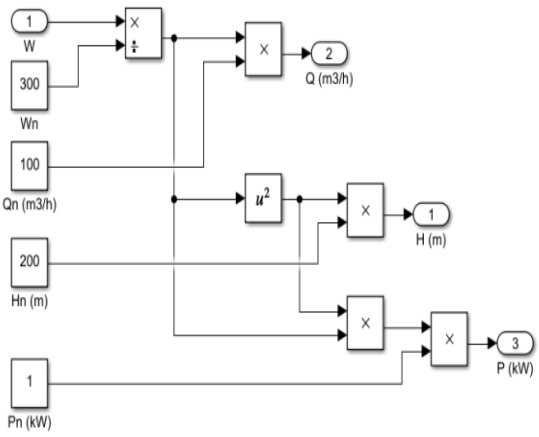

Figure 6. Pump flow chart

Finally, Figure 7 shows the calculation diagram for the water tank, with the water flow rate as input and the water volume and potential energy as output.

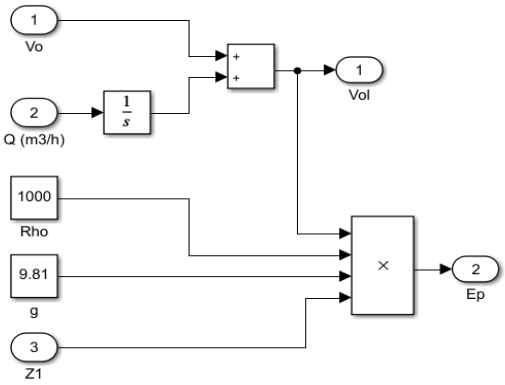

Figure 7. Water tank flow chart

3. Simulation

For the simulation, we used measured values of solar irradiation and temperature (January 24, 2019, in Ouagadougou) [16]. The initial volume of the Vo tank was set at 22.6 m^3 and the final volume, at 1018 m^3 in the case of our study after sizing the reservoir.

The asynchronous motor parameters are given in the table 1.

Table 1. Asynchronous motor parameters

Settings		Values	Units
Stator resistance	r_1	0,12	Ω
Rotor resistance	r_2	0,165	Ω
Magnetizing resistor	rm	224	Ω
Stator leakage reactance	X_1	0,51	Ω
Rotor resistance	X_2	0,45	Ω
Magnetizing reactance	Xm	15,62	Ω
Rated voltage	V	380	V
Pair of poles	P	1	
Synchronizing speed	Nn	2997	rpm
Current	In	44	A
Frequency	fn	50	Hz

The information collected is used to create specific graphs (field power Ppv, absorbed power P_a, water flow Q, water volume V, and potential energy Ep).

4. Results and Discussion

The simulations carried out produced the figures 8 to 13. Figure 8 shows the sunshine and temperature curves used to test the system's operation. Sunshine increases throughout the day, peaking at 12 p.m. and then decreasing to reach its minimum at 6 p.m.

Figure 9 shows the power supplied by the photovoltaic array and absorbed by the motor-driven pump. We can see that the power supplied by the field and absorbed by the motor-driven pump increases proportionally with sunshine, reaching a maximum at solar noon. Both quantities increase from 6 a.m. to 12 p.m. when they reach their maximum values, and then gradually decrease from 12 p.m. to 6 p.m.

We also note that not all the power supplied by the field is absorbed by the motor pump. Intermediate components, such as DC/DC converters or inverters, have losses. Part of the power generated by the PV array is lost as heat.

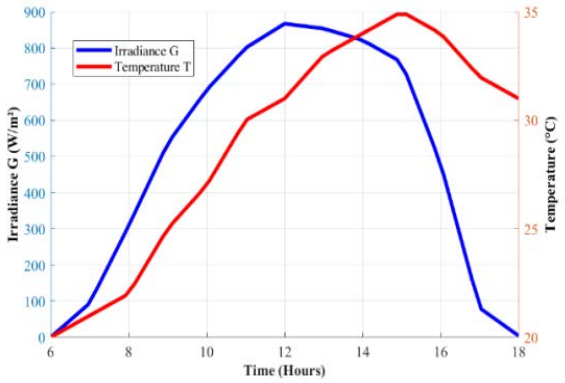

Figure 8. Variations in site illumination and temperature

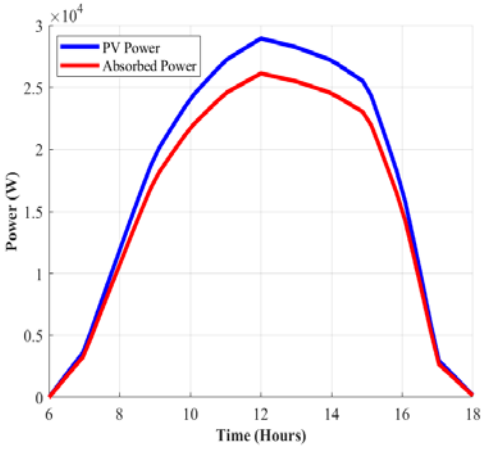

Figure 9. Power generated by the photovoltaic array and absorbed by the motor pump

Figure 10 illustrates the increase in water volume and potential energy from their initial values Vo and Ep(0) to their respective final values (1080 m^3 and 254 MJ). This result demonstrates that the reservoir's potential energy has increased. According to this figure, the final water volume of the reservoir (V_{o1}), which is 1018 m^3, will be reached at around 4:30 p.m. This means that the motor-driven pump can be switched off, and all the power generated by the photovoltaic field can be used directly to supply consumer loads.

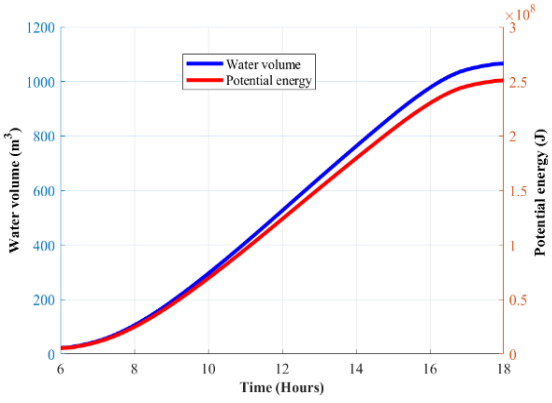

Figure 10. Water volume and potential energy

Figure 11 illustrates the storage of photovoltaic solar energy in the form of potential energy. We see an increase

in the volume of water and its energy potential as a function of fluctuations in solar illumination. This figure illustrates the direct dependency between the operation of the pumping system and variations in solar irradiance. The volume of water pumped and the potential energy increase with the intensity of sunlight, reaching a peak during the sunniest hours before slowing down at the end of the day. This reflects the efficiency of a photovoltaic system adapted to variable energy needs.

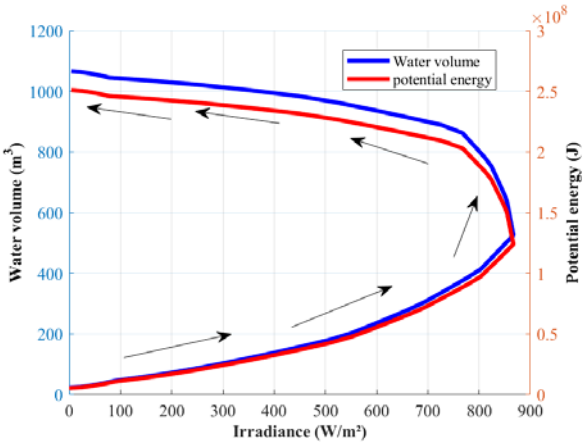

Figure 11. Water volume and potential energy as a function of solar irradiance (arrows indicate the direction of solar irradiance)

The water flow rate is linked to the motor pump rotation speed (laws of similitude), as shown in Figure 12. Moreover, its value varies with solar irradiance, reaching a maximum at 12 p.m. In this system, the pump depends solely on the photovoltaic generator for its flow rate.

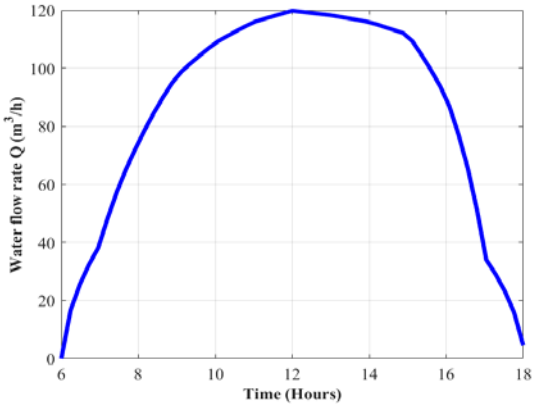

Figure 12. Water Flow Rate

Figure 13 clearly shows that motor pump efficiency varies with solar irradiance. Between 6 a.m. and 12 p.m., the motor pump's efficiency increases significantly. This corresponds to a gradual increase in solar irradiance, which supplies more energy to the system, improving its efficiency. Efficiency peaks (at around 65%) between 12 noon and 2 p.m., corresponding to the peak of sunlight on a typical day. During this period, the pump operates at its optimum level, thanks to abundant photovoltaic power and stable operation. After 2 p.m., output gradually decreases until 6 p.m.. This is due to the reduction in solar irradiance, which limits the power available to the motor pump and reduces its efficiency. The curve has a bell shape, typical of photovoltaic systems coupled to electrical equipment, where efficiency depends directly on light intensity.

At the extremes of the day (6 a.m. and 6 p.m.), efficiency is very low, due to insufficient power to operate the motor pump efficiently.

So, the efficiency of the motor-driven pump is strongly linked to solar irradiance, increasing with the power supplied by the photo voltaic panels and peaking during hours of strong sunlight.

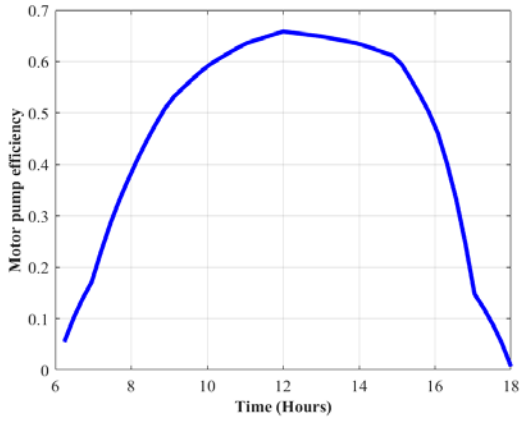

Figure 13. Motor Pump Efficiency

5. Conclusion

In this article, we have presented the modeling of a photovoltaic pumping system, constitued by a photovoltaic field, a motor pump and a water tank, in order to facilitate access to the global simulation of the entire system. Analysis of the various results reveals the direct relationship between photovoltaic solar pumping systems and solar lighting. This work highlights the evolution of motor pump efficiency over time, as a function of solar lighting intensity, reaching a value of 65% at 12 pm.

To the best of our knowledge, previous research has generally been limited to average or static values. The used dynamic method provides a better understanding of immediate changes in performance. The success of this modelling opens the way to practical applications, particularly in remote regions and rural areas where access to water and the electricity grid is limited. This approach not only contributes to a more efficient use of renewable resources, but also to the transition towards a sustainable, environmentally-friendly energy economy. Indeed, system improvement (panel sizing, pump selection, loss control) is essential to optimize efficiency and reliability.

References

[1] R. S. Kookana, P. Drechsel, P. Jamwal, et J. Vanderzalm, «Urbanisation and emerging economies: Issues and potential solutions for water and food security», *Science of the Total Environment*, vol. 732, p. 139057, 2020.

[2] F. Brikké, M. Bredero, W. Supply, et M. Network, «Linking technology choice with operation and maintenance in the context of community water supply and sanitation: A reference document for planners and project staff», A reference document for planners and project staff». World Health Organization and IRC Water and

Sanitation Centre Geneva, Switzerland, 2003. ISBN 92 4 156215 3.

[3] S. Cairncross et V. Valdmanis, «Water supply, sanitation and hygiene promotion (Chapter 41)», In: Jamison DT, Breman JG, Measham AR, et al., editors. Disease Control Priorities in Developing Countries. 2nd edition. Washington (DC): World Bank; 2006. Chap 41.

[4] S. S. Chandel, M. N. Naik, et R. Chandel, «Review of solar photovoltaic water pumping system technology for irrigation and community drinking water supplies», *Renewable and Sustainable Energy Reviews*, vol. 49, p. 1084‑1099, 2015.

[5] S. Meunier, M. Heinrich, J. A. Cherni, L. Quéval, P. Dessante, V. Lionel, A. Darga, C. Marchand et B. Multon «Modélisation et validation expérimentale d'un système de pompage photovoltaïque dans une communauté rurale isolée du Burkina Faso», in *3ème Symposium de Génie Electrique (SGE 2018)*, 2018.

[6] A. I. Imadan, G. C. Semassou, H. A. Saley, L. Sani, et I. D. Boukary, «Dimensionnement et conception d'un système de pompage solaire PV pour le maraichage à ANERSOL au Niger», *Afrique SCIENCE*, vol. 24, n° 2, p. 108‑121, 2024.

[7] D. Abbes, «Contribution au dimensionnement et à l'optimisation des systèmes hybrides éoliens-photovoltaïques avec batteries pour l'habitat résidentiel autonome», *Ecole Nationale Supérieure d'Ingénieurs-Poitiers*, vol. 27, 2012.

[8] R. Nisha et K. G. Sheela, «Review of PV fed water pumping systems using BLDC Motor», *Materials Today: Proceedings*, vol. 24, p. 1874‑1881, 2020.

[9] T. T. Assefa *et al.*, «Evaluating irrigation and farming systems with solar MajiPump in Ethiopia», *Agronomy*, vol. 11, n° 1, p. 17, 2020.

[10] C. S. Guno et C. B. Agaton, «Socio-economic and environmental analyses of solar irrigation systems for sustainable agricultural production», *Sustainability*, vol. 14, n° 11, p. 6834, 2022.

[11] M. T. Ejigu, «Solar-powered pump drip irrigation system modeling for establishing resilience livelihoods in South Omo zone and Afar regional state, Ethiopia», *Model. Earth Syst. Environ.*, vol. 7, n° 1, p. 511 ‑ 521, mars 2021, doi: 10.1007/s40808-020-00927-2.

[12] R. B. Silva, I. Teodoro, J. L. de Souza, R. A. Ferreira, M. A. dos Santos, et G. M. C. Martins, «Water balance and technical-financial performance of irrigation in the cassava cultivation», *Revista Ceres*, vol. 70, n° 5, p. e70507, 2023.

[13] M. Belhadj, T. Benouaz, A. Cheknane, et S. M. E. A. Bekkouche, «Estimation de la puissance maximale produite par un générateur photovoltaïque», *Journal of Renewable Energies*, vol. 13, n° 2, p. 257‑264, 2010.

[14] M. Thiam, O. Dia, M. Diop, G. Sow, L. Thiaw, D. Azilinon et O. Diao, «Détermination des paramètres du modèle à une diode d'un module photovoltaïque», *Afrique SCIENCE*, vol. 12, n° 3, p. 77‑83, 2016.

[15] D. Mitrushi, «Apport d'une station de transfert d'énergie par pompage sur le taux d'intégration des EnR», PhD Thesis, Université Pascal Paoli, Universiteti politeknik i Tiranës. Albanie, 2016.

[16] Éric Simonguy, «Dimensionnement, modélisation et optimisation d'un système PV avec stockage hydraulique destiné à la production d'électricité en site isolé», Thèse de doctorat, Université Joseph Ki-Zerbo, Burkina Faso, 2019.

[17] T. T. Guingane, Z. Koalaga, E. Simonguy, F. Zougmore, et D. Bonkoungou, «Modélisation et simulation d'un champ photovoltaïque utilisant un convertisseur élévateur de tension (boost) avec le logiciel MATLAB/SIMULINK», *Journal International de Technologie, de l'Innovation, de la Physique, de l'Energie et de l'Environnement*, vol. 2, n° 1, 2016.

[18] D. Spirov, V. Lazarov, D. Roye, Z. Zarkov, et O. Mansouri, « Modelisation Des Convertisseurs Statiques Dc-Dc Pour Des Applications Dans Les Energies Renouvelables En Utilisant Matlab/Simulink® », *EF 2009, Compiegne*, 2009.

[19] M. Muselli, G. Notton, P. Poggi, et A. Louche, « PV-hybrid power systems sizing incorporating battery storage: an analysis via simulation calculations », *Renewable Energy*, vol. 20, n° 1, p. 1‑7, 2000.

[20] A. Betka et A. Moussi, «Performance optimization of a photovoltaic induction motor pumping system», *Renewable energy*, vol. 29, n° 14, p. 2167‑2181, 2004.

[21] J. M. D. Murphy et F. G. Turnbull, *Power electronic control of AC motors*, 1st ed. Oxford [Oxfordshire] ; New York: Pergamon, 1988.

[22] N. Hidouri et L. Sbita, «Water photovoltaic pumping system based on DTC SPMSM drives», *Journal of Electric Engineering: Theory and Application*, vol. 1, n° 2, p. 111‑119, 2010.

[23] E. Simonguy, E. Korsaga, J. M'boliguipa, T. T. Guingané, et Z. Koalaga, «Performance of photovoltaic pumping station using a centrifugal motor-pump working at fixed speed», International Journal of Engineering &Technology, vol. 7, n° 4,p. 7021-7027 ,2018, doi: 10.14419/ijet.v7i4.16825.

[24] H. Suehrcke, J. Appelbaum, et B. Breshef, «Modelling a permanent magnet DC motor/centrifugal pump assembly in a photovoltaic energy system», *Solar energy*, vol. 59, n° 1‑3, p. 37‑42, 1997.

[25] M. Alonso Abella, E. Lorenzo, et F. Chenlo, «PV water pumping systems based on standard frequency converters», *Progress in Photovoltaics*, vol. 11, n° 3, p. 179‑191, mai 2003.